IAES International Journal of Artificial Intelligence (IJ-AI)
Vol. 15, No. 6, December 2026, pp. 5774∼5787
ISSN: 2252-8938, DOI: 10.11591/ijai.v15.i6.pp5774-5787

Deep learning framework for nuchal translucency thickness measurement and down syndrome detection

Sandip Rajendra Aher[1,2,3], Balasaheb Shrirangrao Agarkar[1,2], Sachin Vasant Chaudhari[1,2]
[1]Department of Electronics and Telecommunication Engineering, Sanjivani College of Engineering, Kopargaon, India
[2]Department of Electronics Engineering, Savitribai Phule Pune University, Pune, India
[3]Department of Electroncs and Telecommunication Engineering, Pravara Rural Engineering College, Loni, India

Article Info

Article history:

Received Oct 17, 2025
Revised Aug 17, 2026
Accepted Sep 20, 2026

Keywords:

Deep learning
Down syndrome
Ensemble learning
Nuchal translucency
You only look once version 8

ABSTRACT

The nuchal translucency (NT) region in fetal ultrasound images can be measured to screen for down syndrome (DS), a common chromosomal disorder, in the early stages of pregnancy. However, operator bias and variability can affect manual assessment. In this study proposed an automated deep learning framework that integrates you only look once version 8 (YOLOv8)-based NT localization with bounding box-based thickness estimation and ensemble classification. The YOLOv8 was selected for its ability to detect fine anatomical regions. The NT region is first automatically localized and then cropped using YOLOv8, allowing for consistent region of interest (ROI) delineation. An ensemble classifier combining residual network-50 (ResNet50), densely connected convolutional network-201 (DenseNet201), and efficient neural network-B4 (EfficientNet-B4) with soft voting is trained on these labeled images for reliable and sensitive DS risk classification. The YOLOv8 detector achieved excellent NT localization performance, achieving mAP@50 of 94.7%, precision of 92.3%, and recall of 88.4%. Experimental results for classification using an ensemble classifier achieve 98.10% accuracy, outperforming traditional methods. Through the integration of detection with clinically interpretable NT thickness measurement, the framework offers a viable tool for early and accurate DS screening in everyday clinical practice.

This is an open access article under the CC BY-SA license.

Corresponding Author:

Sandip Rajendra Aher
Department of Electronics and Telecommunication Engineering, Sanjivani College of Engineering
Kopargaon, India
Email: sandip.aher1719@gmail.com

1. INTRODUCTION

The nuchal translucency (NT) sonography has become a valuable tool in the early diagnosis of down syndrome (DS). The DS results from trisomy 21, an extra copy of chromosome 21, and is the most common viable autosomal aneuploidy [1]. It remains a major cause of intellectual disability and congenital anomalies worldwide. Over the past century, numerous epidemiological studies have investigated its prevalence and clinical implications. While the reported incidence varies across populations, in the United States, DS occurs in roughly one out of every 700 live births [2]. Ultrasonography's non-invasive, cost-effective, and continually improving imaging quality make it a popular choice for fetal identification and inspection [3]. Both prenatal and postnatal detection of DS are possible. Ultrasound examination and biochemical serum analysis are part of prenatal screening [4]. The intrusive diagnostic procedures like chorionic villus sampling and amniocentesis

may result in miscarriage and fetal harm in the search for DS. The DS indicators, such as NT and nasal bone (NB), are visible in early trimester scans and can be combined with serum markers for higher accuracy [5].

The DS screening in the first trimester was derived from NB evaluation [6]. Evaluating NT measurements has proven effective in the early screening of major chromosomal disorders, including trisomy 13, 18, and 21 [7], [8]. The fluid-filled area in the posterior aspect of the fetal neck, beneath the skin, is known as the NT [9]. The epidermis appears white (echogenic), while the NT fluid beneath the skin has a black (anechogenic) appearance. Between weeks eleven and fourteen of pregnancy, it is evaluated. At the fourteenth week of pregnancy, NT usually goes away [10]. For the NT calculation, the fetus's crown-rump length must be between 45 mm and 84 mm [11]. A hereditary problem may arise from an enlarged NT that is thicker than 3.5 mm, increasing the risk of cardiac abnormalities associated with DS [12]–[15].

To properly test NT, the fetus needs to be visible in the mid-sagittal view. Using the electronic caliper, the doctor determines the thickness of NT on their own [16]. To finish the calibration, the caliper is placed between the two distinct echogenic lines that are shown on the screen. The thickness of the NT is within a few millimeters, so it needs to be measured with care, or else it might give a significant diagnostic error. This means automation decreases the risk of human error and will provide consistent measurement. The NT examination is an important component of computer-aided diagnosis (CAD) for the early detection of DS. The major disadvantages of the conventional localization methods include indistinct edges, consistent intensity, longer processing time, and the increased chances of error when recovering the NT region. Eliminating these hurdles, an automated system for DS detection would result in a faster and more accurate diagnosis of the fetus. Distinguishing the NT images from the ultrasound images is a challenge. There is a strong overlap between the intensity patterns of NT zones and the surrounding background regions. Additionally, when the fetus rotates, the NT area's anatomy changes dramatically. The segmentation process is made more difficult by the inherent differences in ultrasonic intensity between organizations, scanners, and operators [17].

This study anticipate an increasing prevalence of NT sonography-based screening programs for the general public. However, this study must resolve a few practical implementation issues before approves the widespread use of this strategy. Advanced sonographer skills are required for the evaluation of the NT, so the Fetal Medicine Foundation (FMF) created a protocol defining these requirements to ensure precise measurement [18]. A precise evaluation of NT thickness is a clinically relevant indicator in fetal diagnosis to detect chromosomal disorders like DS. Traditional manual methods for determining NT thickness in fetal ultrasound images can be laborious and subjective, leading to inconsistent results. This motivates us to present a useful tool for automatic NT measuring that will aid in early diagnosis of DS, also incorporating classification of normal and DS fetuses.

The you only look once version 8 (YOLOv8) architecture has gained increasing popularity in recent years due to its attractive features in terms of speed, accuracy, and architecture properties, making it ideally suitable for ultrasound image analysis [19]. More specifically, it is single-stage, anchor-free design simplifies the detection process, and it allows for real-time inference, which is an important requirement for potential clinical integration. In addition, it has powerful multi-scale feature fusion capabilities due to its advanced backbone and neck networks, which include a cross stage partial darknet (CSPDarknet) encoder and a feature pyramid network (FPN) with a path aggregation network (PAN). This is essential for detecting small low-contrast objects in complex and noisy background scenes. These characteristics directly relate to the challenges of NT segmentation. The multi-scale processing capability of the model enables the model to accurately detect the fine echogenic lines representing the NT membrane for different fetal poses and fetal ages. Furthermore, its recall value is high and it minimizes the chance of failing to detect the entire NT, and the bounding box regression is very precise and optimized with a complete intersection over union (CIoU) loss function to ensure the initial region of interest (ROI) is well cropped. This is an accurate detection that is a basic prerequisite for the subsequent segmentation and classification stage, it will allow the ensemble model to analyze the structure they are looking for and thus increase the robustness and reliability of the proposed screening framework.

The YOLOv8 [20] framework is used in this study to precisely localize the NT region in fetal ultrasound pictures, allowing for reliable identification even in the presence of poor contrast and changing imaging quality. Unlike previous models such as faster region-based convolutional neural network (Faster R-CNN) and YOLOv5, the selection of YOLOv8 was made for its powerful backbone and decoupled detection head, which boosts the accuracy, inference speed, and generalization capabilities. Transfer learning is applied to an ensemble of residual network-50 (ResNet50) [21], densely connected convolutional network-201

(DenseNet201) [22] and efficient neural network-B4 (EfficientNet-B4) [23] for DS risk classification. These models were chosen because of the complementary strengths. Residual connections in ResNet50 greatly simplify the learning of deep networks by reducing vanishing gradients and thus facilitating good feature extraction. This innovative compound scaling approach optimises model accuracy and minimises computation resources to achieve the best of both worlds in the EfficientNet-B4. The DenseNet201 is an architecture of dense connectivity which further improves the gradient flow across the network and encourages feature re-use across layers. These three models are combined into an ensemble architecture to get diverse feature representations, reduce overfitting and enhance generalization for diverse ultrasound scans. This can increase the sensitivity and specificity to achieve reliable and consistent diagnosis of DS in prenatal screening.

The novelty of the proposed framework lies in the integration of YOLOv8-based NT localization with an ensemble of ResNet50, DenseNet201, and EfficientNet-B4 for DS classification. YOLOv8 enables accurate NT region detection, while the ensemble exploits complementary feature representations to improve classification accuracy, robustness, and generalization. This synergistic combination provides a more reliable framework for automated prenatal DS screening. The main contributions of this study are as follows: i) proposal of novel YOLOv8-based approach for locating the NT area precisely in the fetal ultrasound images; ii) automatic NT thickness approximation from YOLOv8 detected ROI; and iii) the ensemble learning method employs ResNet50, DenseNet201, and EfficientNet-B4 for classification and DS risk assessment.

This paper is structured as follows: the introduction is covered in section 1. The related work is covered in section 2, and the proposed framework for locating NT regions and classifying DS is covered in section 3. The findings and discussion of the proposed framework are presented in section 4. Finally, the study's conclusion and future scope are discussed in section 5.

2. RELATED WORK

The NT measurement is the subject of much research in the literature, including Bernardino *et al.* [16], who made one of the first attempts to automate the process. Since the membranes surrounding the translucency must be manually identified, their method is semi-automatic; they serve as the beginning locations for tracing around the edges through Canny and Sobel filters. In general, this method underestimates the NT's thickness in comparison to a doctor's verified ground truth. Applications of the method are limited to images in which the fetus is horizontal. Catanzariti *et al.* [24] refined the cost function to segment the borders that define translucency, avoiding the need for beginning values. The sonography pictures have been pre-processed using a median filter by Nirmala and Palanisamy [25] to remove speckle noise. Then, they used the mean shift technique to segment the regions that included the NT. The Canny operator is then applied to the segmented images to draw the boundaries defining the NT. Furthermore, a mathematical contrast between the mean thickness values for normal and typical translucency has been presented.

A semi-automatic method was introduced by Deng *et al.* [26], in which morphological filtering is used to reduce noise in images before an experimentally established threshold is used. They choose two starting spots, and the gradient vector flow technique is used to estimate the edges from these points. A dynamic programming process then refines the edges to obtain the NT's thickness and area. In an additional investigation, Deng *et al.* [27] introduced a hierarchical framework for identifying the nuchal area, where three support vector machine (SVM) classifiers were used to separate the fetal head, neck, and body regions. By adding a layer to the structural model to represent the fetal profile, Deng *et al.* [28] improved performance by reusing the same approach.

Some ultrasound devices integrate and promote the sonography-based nuchal translucency (SonoNT) architecture, which was first presented by Moratalla *et al.* [7]. With this tool, NT can be evaluated semi-automatically by having the user draw a box that contains the maximum thickness for the NT. This tool uses the gradient and brightness values inside the box to monitor the top and lower edges, then calculates the maximum gap between them. Supriyanto *et al.* [29] processed image sub-samples and calculated correlation values for NT classification using a multilayer neural network. The borders of NT regions were drawn by an automated technique based on pixel intensity. Park *et al.* [30] determined both the outer and inner bounds of the two distinct components that constitute the translucency using Dijkstra's approach. They used the segmentation graphs cut process after choosing seed points within these specific areas.

Thereafter, the NT's diameter is evaluated. The NT thickness and edge extraction qualitative ratings are graphically represented, showing five of the best and worst cases. Sonia and Shanthi [31] used an SVM

and discrete wavelet transform (DWT)-based feature extraction to detect DS. This approach has drawbacks, including the inability to objectively determine NT thickness, identify edges, and evaluate maximum thickness. Anzalone *et al.*'s study [32] used an automated method to quantify NT by first identifying the medial sagittal plane and then assessing the thickness of NT in the nuchal area. Thomas and Arjunan [33] employed convolutional neural network (CNN)-driven segmentation network (SegNet) architecture based on visual geometry group 16 (VGG-16) to semantically divide the NT region in fetal ultrasound pictures.

Chaudhari and Oza [34] state that an automated framework incorporating a generalized regression neural network (GRNN) and scale-invariant feature transform (SIFT) features for crucial point extraction was used to evaluate NT thickness. Devi and Ramachandran [35] claimed that the adaptive boosting (AdaBoost) algorithm worked well for NT region recognition. Adding to this, Liu *et al.* [36] used a CNN with fully linked layers to identify the NT region and created a specially designed U-network (U-Net) framework with a particular loss function to accomplish accurate NT segmentation. Aher *et al.* [37] proposed the deep learning methodology for early DS identification using GoogLeNet and AlexNet. The GoogLeNet was used for precise localization, while AlexNet was used for classification. Zhang *et al.* [38] created a CNN to create a deep learning model. They utilized data augmentation to produce additional data.

Various groups were randomly chosen as training and validation sets to evaluate the resilience of the deep learning model. Kasera *et al.* [39] focuses on the automated recognition of the NT measurement as a foundational step toward detecting more complex fetal anomalies. While clinical diagnosis of an increased NT relies on an absolute measurement in millimeters at a specific gestational age, their method quantifies it as a ratio of the NT region area to the fetal region area. Liu *et al.* [40] introduced a fusion model that amalgamated the benefits of radiomics, CNN, and vision transformers (ViT) for the intelligent evaluation of ultrasound pictures in NT measurement. To overcome image quality and positional relation, and time-consuming data collection and detailed annotation issues, Zhao *et al.* [41] introduced a framework on the basis of densely connected convolutional network (DenseNet) model.

Chen *et al.* [42] developed a transfer learning model based on the AlexNet architecture. Do *et al.* [43] created predictive models for the first and second trimesters of pregnancy using three sets of different variables and compared these models, intending to find the best model in each trimester based on the combination of sensitivity and specificity that maximizes these scores while requiring the least amount of information. To provide standardized NT images that meet the criteria and to aid in assessment of the fetus during pregnancy, Zhang *et al.* [44] developed an artificial intelligence (AI)-based model called the automated identification and measurement of nuchal translucency (AIM-NT). Kwon *et al.* [45] proposed an automatic recognition method for the standard mid-sagittal plane in three dimensional ultrasound volumes using a deep learning network, which demonstrated good reproducibility and reduced subjectivity dependency in the evaluation of NT. Baddad *et al.* [46] proposed a dual-phase deep learning approach to the evaluation of NT regions. A DenseNet121 model is first used to assess picture quality and remove those not following regular standards, and then a DenseNet/segmentation system is used to segment the NT region for automatic assessment.

3. PROPOSED METHOD

The block diagram of the proposed framework for NT detection and classification of DS with YOLOv8 and ensemble learning is shown in Figure 1. The proposed framework is divided into four major phases: preprocessing of input fetal ultrasound images, NT region detection using YOLOv8, NT cropping and thickness measurement, and ensemble learning using ResNet50, DenseNet201, and EfficientNet-B4 to predict DS. The preprocessing techniques are applied to fetal ultrasound images in the first stage in order to enhance image clarity and diversify the dataset. The NT region is automatically localized in the second stage using the YOLOv8 detector, guaranteeing precise and reliable ROI extraction over a range of image quality. The detected region of the NT is then cropped and passed on to the measurement stage.

In the third step, the thickness of the ROI is cropped and the greatest vertical distance (in mm) is used to determine the NT thickness. The clinical criteria defined were used to classify the babies with NT thickness under 3.5 mm as healthy and the babies with NT thickness ($\geq$ 3.5 mm) as DS. This auto-labeling procedure guarantees uniformity and gets rid of manual dependency. The last step involves training an ensemble classifier made up of ResNet50, DenseNet201, and EfficientNet-B4 using the labeled datasets. Ensemble of all architectures with soft voting technique increases the reliability and robustness of classification when compared to individual architectures.

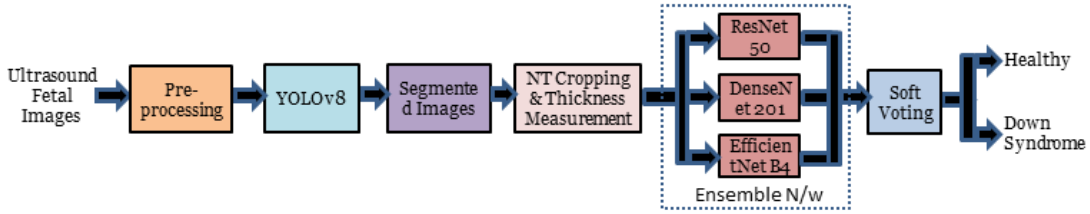

Figure 1. The proposed framework for NT region localization and DS classification

3.1. Dataset

For this study uses a publicly available Fetus framework dataset from the Mendeley Data [47]. This dataset comprises 1,528 two-dimensional sagittal-view ultrasound scans of 1,519 females obtained from Shenzhen People's Hospital. Prior to model development, all images underwent a quality assessment based on predefined inclusion criteria. Images with poor ultrasound quality, incomplete visualization of the NT region, duplicate records, or missing/inconsistent annotations were excluded. Consequently, 1,325 high-quality images were retained for this study. The dataset contains an inherent imbalance between healthy and DS samples, with healthy cases forming the majority class. To address this issue, this study adopted a multi-level imbalance mitigation strategy. Class-weighted loss functions were applied during DS classification to penalize minority class errors more strongly. Additionally, augmentation-based oversampling was performed on DS samples to enhance minority class representation. For NT region detection, YOLOv8's focal loss was utilized to reduce dominance of majority samples. These techniques collectively improved model robustness and sensitivity to DS cases. For the YOLOv8-based NT localization task, the selected dataset was randomly divided into 927 training images (70%), 265 validation images (20%), and 133 testing images (10%). All retained images annotations are imported from dataset with bounding boxes around the NT region. The same dataset was subsequently used to generate NT ROI images for the ensemble-based DS classification framework. The five-fold cross-validation was employed for the classification stage to enhance generalizability and reduce bias.

3.2. Pre-processing

The sonographic fetal image is influenced by noise distortion, which degrades the sharpness of local features. The proposed approach utilizes an anisotropic diffusion filter (ADF) to diminish image noise [37], [18]. The ADF eliminates high-frequency interference while maintaining the fundamental outlines of current objects.

3.3. Nuchal translucency region of interest localization using you only look once version 8

This study uses the YOLOv8 framework for the NT region detection. The architecture of YOLOv8 is shown in Figure 2. It is based on a one-stage detection pipeline that is optimized for speed and accuracy in medical image analysis [39]. The whole framework consists of four sections: the input layer, the backbone, the neck, and the prediction head. Grayscale ultrasound fetal images are inputted into the input module which is designed to prepare them for feature extraction. The backbone network is built based on convolutional (Conv) layers and cross-stage partial connections (C2F), which is able to learn hierarchical features, gathering low-level texture features, and high-level semantic features. Moreover, the spatial pyramid pooling–fast (SPPF) block can be used to handle images of various scales of fetuses [19]. Neck module is the concatenation and upsampling of different scales of features, improving the contextual information of small area such as NT area. Finally, the prediction head provides a detection result in various scales, which specially points to the NT region with high accuracy. The YOLOv8 detection head was used to detect the NT bounding box and accurately identify the ROI. The YOLOv8 model's lightweight design makes it more efficient for real-time ultrasound image processing and clinical use without compromising detection accuracy.

Let an input image be I and let the network predict outputs at S spatial scales. At a given scale with stride s, the network outputs a tensor of shape (H_s, W_s, C) where each spatial cell (i, j) predicts a vector of values for a candidate object, as in (1).

$$P_{i,j} = (t_x, t_y, t_w, t_h, o, c) \in \mathbb{R}^{4+1+K} \tag{1}$$

Where t_x, t_y, t_w, t_h are bounding-box parameterizations, o is the objectness logit, $c \in \mathbb{R}^K$ are class logits, and K is the number of classes [20].

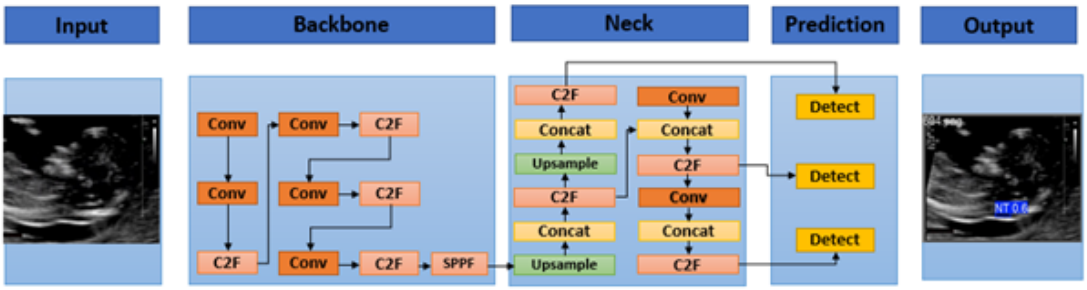

Figure 2. The NT ROI localization using YOLOv8

Bounding-box decoding from network outputs to image coordinates uses a cell offset (c_x, c_y) and stride s. A standard decode is in (2) to (5).

$$b_x = \frac{\sigma(t_x) + c_x}{W_s} \tag{2}$$

$$b_y = \frac{\sigma(t_y) + c_y}{H_s} \tag{3}$$

$$b_w = \frac{\exp(t_w)}{W_s} \tag{4}$$

$$b_h = \frac{\exp(t_h)}{H_s} \tag{5}$$

Where $\sigma(\cdot)$ is the sigmoid function; $(b_x, b_y, b_w,$ and $b_h)$ are normalized center and size in image coordinates (or multiplied by image width/height to obtain pixel values). Objectness and class probabilities are obtained via sigmoid/softmax, as in (6) and (7).

$$\hat{o} = \sigma(o) \tag{6}$$

$$\hat{p} = \text{softmax}(c) \tag{7}$$

Predictions from all spatial scales are concatenated and then post-processed by confidence thresholding and non-maximum suppression (NMS) to yield final detections. The YOLOv8 loss function is a weighted combination of bounding-box regression, objectness prediction, and classification losses to jointly optimize accurate localization and reliable detection, as in (8).

$$L = \lambda_{\text{box}} L_{\text{box}} + \lambda_{\text{obj}} L_{\text{obj}} + \lambda_{\text{cls}} L_{\text{cls}} \tag{8}$$

Where L_{box} is bounding-box loss, L_{obj} is objectness loss, and L_{cls} is classification loss.

This study used the YOLOv8 model for localization, which was trained on the pre-processed data using 30 epochs, a batch size of 16, and input size of 640 × 640 pixels. The pretrained weights were used to initialize the model, and an initial learning rate of 0.01, a momentum of 0.937, and a weight decay of 0.0005 were used for optimization. Data augmentation was applied only to the training dataset, while the validation and test datasets were kept unchanged to ensure an unbiased evaluation of the model. Extensive augmentation techniques, including horizontal flipping, mosaic augmentation, random scaling, translation, hue, saturation, and value (HSV) color modifications, and random erasing, were employed to increase robustness against variations in fetal orientation, image scale, illumination, and ultrasound acquisition conditions. These augmentation strategies improved dataset diversity, reduced overfitting, and enhanced the model's generalization capability, thereby contributing to improved localization performance on unseen ultrasound images.

The model's hyperparameters were determined by empirical adjustment according to validation outcomes. The many permutations of learning rate, batch size, and training epochs were evaluated to ascertain the optimal training setup. The learning rate was explored from 0.00001 to 0.1, batch size of 8, 16 and 32,

and number of epochs from 20 to 70. Finally, stable convergence, minimized validation loss, and enhanced validation accuracy were considered to ensure model stability, efficiency, and generalization. Because of its stable convergence and effective optimization performance on medical imaging datasets, the adaptive moment estimation with decoupled weight decay (AdamW) optimizer [48] was chosen. The final hyperparameter settings used for the training of the YOLOv8 model are given in Table 1.

Table 1. Final training hyperparameters and configuration of the proposed YOLOv8 model

Parameter	Value/setting
Input size	640 × 640 pixels
Optimizer	AdamW
Initial learning rate	0.01
Learning rate schedule	Cosine annealing
Momentum (β_1)	0.937
Weight decay	0.0005
Batch size	16
Number of epochs	30
Random seed	42

3.4. Nuchal translucency thickness measurement and label assignment

After localizing the NT region using the YOLOv8 model, the bounding box coordinates were extracted to precisely localize the ROI. The maximum vertical span within the detected ROI was approximated as NT thickness, assuming bounding box boundaries align with echogenic lines. While this approach does not provide pixel-level segmentation, it offers a practical and standardized proxy for thickness measurement. This pixel-based measurement was then converted into millimeters using a calibration factor derived from the ultrasound imaging system, ensuring clinical relevance of the measurements. The measured thickness values were used to crop the NT region. The cropped NT images are classified as either healthy or DS fetuses based on thickness threshold values as described earlier. These images are then utilized as input features for an ensemble-based classifier.

3.5. Prediction of down syndrome using ensemble network

To achieve robust and reliable classification of cases (healthy vs. DS) based on NT measurements and DS prediction, an ensemble deep learning framework was developed by integrating three networks: ResNet50, DenseNet201, and EfficientNet-B4. The proposed pipeline employs a 5-fold stratified cross-validation strategy, ensuring balanced evaluation across classes and mitigating bias from data imbalance. Data augmentation techniques such as random cropping, rotation, horizontal flipping, and color jittering were applied to increase generalization capability, while a weighted random sampler was utilized to counter class imbalance during training. This study used random rotation and flips to simulate fetal position variations. Data was split before augmentation to prevent leakage. Each fold contained balanced proportions of healthy and DS cases. Each backbone network was trained independently with AdamW optimization and cosine annealing learning rate scheduling, followed by early stopping. Predictions from the three networks were combined through a soft voting ensemble mechanism, where class probabilities were averaged to yield the final decision. This study used equal weights for soft voting since all three models achieved similar validation performance.

In the proposed ensemble strategy, each backbone model $m \in \{1, 2, 3, \ldots, M\}$ generates a posterior probability distribution over K classes for sample i, as in (9).

$$p_m^{(i)} = \left(p_{m,1}^{(i)}, \ \ldots, \ p_{m,K}^{(i)}\right), \quad \sum_{k=1}^{K} p_{m,k}^{(i)} = 1 \tag{9}$$

To enhance robustness and reduce model-specific bias, predictions are aggregated through soft voting, where the ensemble probability is obtained as (10).

$$\bar{p}^{(i)} = \frac{1}{M} \sum_{m=1}^{M} p_m^{(i)} \tag{10}$$

This probabilistic fusion of networks utilize the complementary strengths of all architectures, providing more stable predictions. This ensemble strategy exploits the complementary feature learning

capabilities of diverse architectures, leading to improved stability and diagnostic accuracy compared to individual models, thereby reducing variance and bias. Thus, through this NT region's measurements and the ensemble network, the fetus is classified as healthy or DS.

4. RESULTS AND DISCUSSION

The present study developed and evaluated a novel framework for the automated detection of NT and subsequent screening for DS in prenatal ultrasound images. This section quantitatively assesses the performance of the proposed system, which integrates a YOLOv8 object detector for precise NT localization with an ensemble classifier for robust risk classification. The representative outcomes of the suggested YOLOv8 framework for automated NT localization in fetal ultrasound images are displayed in Figure 3. The model's certainty is indicated by confidence ratings (0.3 – 0.7), which are lower (0.3) in difficult situations like noise or fetal movement and higher($\geq$ 0.6) in obvious scenarios. These findings show that the model has the potential to increase the dependability of NT-based DS screening and show consistent performance across imaging differences.



Figure 3. YOLOv8-based detection of the NT region with confidence scores

The YOLOv8 detector yielded high accuracy in NT localization, with a precision of 92.3%, a recall of 88.4%, and an mAP@50 of 94.7%. These results surpass conventional segmentation and structural approaches [27], [47] and are competitive with earlier deep learning models [27], [37], demonstrating YOLOv8's effectiveness in accurately localizing the NT region. The confusion matrix illustrating the classification outcomes is presented in Table 2. The model correctly classified 98.57% of healthy fetuses and 97.64% of DS cases, with only minimal misclassifications. The balanced classification accuracy achieved was 98.10%, indicating that the system proved reliable and clinically applicable in identifying subtle structural differences within the NT region. The ensemble is reliable enough for clinical support.

Table 2. Evaluation results

Actual class	Predicted class	
	Healthy	DS
Healthy	98.57	1.43
DS	2.3	97.64
Accuracy	98.10	

The performance of the proposed ensemble framework for binary classification is comprehensively summarized in Table 3. The model demonstrated high accuracy, with robust metrics confirmed through

5-fold cross-validation (mean ± standard deviation), where the class distribution of healthy and DS cases was preserved in each fold to ensure balanced training and evaluation. The consistent performance across all folds demonstrates the robustness of the proposed framework under balanced class distributions.

The proposed framework achieved an overall accuracy of 98.1%, with a high receiver operating characteristic-area under the curve (ROC-AUC) of 0.996, indicating excellent discriminative capability between healthy and DS fetuses. For the DS class, the model achieved a recall of 97.6%, which is particularly important in prenatal screening applications. For the healthy class, the proposed framework achieved a precision of 98.4%, a recall of 98.5%, and an F1-score of 99.1%, demonstrating reliable identification of normal fetuses with a very low false-positive rate. These class-wise results confirm that the proposed ensemble framework maintains strong and balanced performance across both classes while prioritizing high sensitivity for DS detection, which is desirable for clinical decision-support systems. Furthermore, this study performed a statistical significance test with 95% confidence interval to validate the proposed ensemble framework over the best-performing individual baseline model. A paired t-test conducted on the ROC-AUC scores from the five folds yielded a p-value of $p < 0.01$, indicating that the performance improvement afforded by the ensemble is statistically significant.

Table 3. Five-fold cross-validation results of the proposed ensemble framework (mean ± standard deviation)

Metric	Value
Overall accuracy	0.981 ± 0.04
Recall-DS class	0.976 ± 0.07
Precision-DS class	0.836 ± 0.09
F1-score-DS class	0.903 ± 0.12
Recall-healthy class	0.985 ± 0.08
Precision-healthy class	0.984 ± 0.05
F1-score-healthy class	0.991 ± 0.07
ROC-AUC	0.996 ± 0.03

Table 4 compares analysis of the classification performance of individual deep learning models, two-model ensembles, and the proposed three-model ensemble approach. The proposed YOLOv8 + ensemble method, which combines the complementary predictive capabilities of ResNet50, DenseNet201, and EfficientNet-B4, achieved accuracy of 98.10%, with a DS-class precision of 83.65%, recall of 97.64%, and F1-score of 90.35%. The high recall demonstrates the ability of the proposed framework to correctly identify the majority of DS cases, which is particularly important in prenatal screening applications. The corresponding F1-score confirms the robustness of the proposed ensemble framework for DS classification. The results show that the proposed YOLOv8 + ensemble model outperformed all individual models and two-model ensemble combinations across all evaluated metrics.

Table 4. Comparison of classification performance for various model combinations

Model	Accuracy (%)	Precision-DS(%)	Recall-DS(%)	F1-score-DS (%)
YOLOv8 + ResNet50	92.13	79.22	93.18	87.35
YOLOv8 + DenseNet201	93.65	80.39	95.67	87.94
YOLOv8 + EfficientNet-B4	95.95	80.76	94.23	88.16
YOLOv8 + ResNet50 + DenseNet201	96.09	81.36	95.52	88.8
YOLOv8 + DenseNet201 + EfficientNet-B4	97.11	83.10	96.91	89.32
YOLOv8 + ResNet50 + EfficientNet-B4	96.56	82.47	95.76	88.09
YOLOv8 + ensemble (proposed)	98.10	83.65	97.64	90.35

Among the individual models, YOLOv8 + EfficientNet-B4 achieved the highest accuracy of 95.95%, followed by YOLOv8 + DenseNet201 and YOLOv8 + ResNet50. The two-model ensembles further improved the performance, achieving accuracies of 96.09%, 96.56%, and 97.11% for YOLOv8 + ResNet50 + DenseNet201, YOLOv8 + ResNet50 + EfficientNet-B4, and YOLOv8 + DenseNet201 + EfficientNet-B4, respectively. Notably, the YOLOv8 + DenseNet201 + EfficientNet-B4 combination achieved the highest accuracy among the two-model ensembles, with a DS-class precision of 83.10%, recall of 96.91%, and F1-score of 89.32%. Finally, integrating all three models produced the best overall performance, demonstrating that combining complementary feature representations improves classification accuracy, enhances the detection of DS cases, reduces model variance, and improves generalization compared with individual models and two-model ensemble configurations.

The gradient-weighted class activation mapping (Grad-CAM)-based explainability of the YOLOv8 NT detection model is shown in Figure 4. The Grad-CAM was applied to the detection head using objectness confidence gradients, and the resulting activation maps consistently highlight the NT region across ultrasound images. Figure 4(a) shows the original ultrasound image, while Figure 4(b) illustrates the YOLOv8-predicted bounding box for NT localization. Figure 4(c) presents the corresponding Grad-CAM heatmap, highlighting the regions contributing to the model's detection response. The activation map demonstrates that the model's highest responses are concentrated within the predicted NT region along the posterior fetal neck, while surrounding anatomical structures exhibit minimal activation. This alignment between the detected NT region and Grad-CAM activations indicates that the model's predictions are influenced by clinically pertinent anatomical features rather than background artifacts. This improves transparency and supports real-world clinical applicability.

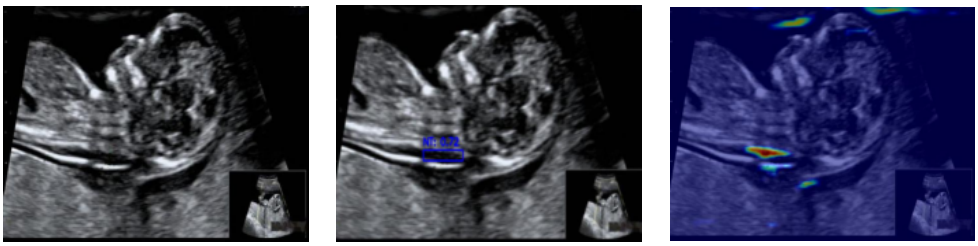

(a) (b) (c)

Figure 4. Grad-CAM visualization of the proposed YOLOv8 model for NT region detection of (a) original ultrasound image, (b) detected NT bounding box, and (c) Grad-CAM heatmap showing model attention concentrated within the NT region

Table 5 provides a comprehensive performance comparison between the proposed YOLOv8 and ensemble-based framework and several existing state-of-the-art methods for NT analysis and DS screening. Traditional methods such as the Chan-Vese–based segmentation model and the hierarchical structural model achieved accuracies of 90% and 94%, respectively, while earlier deep learning models like deep neural networks (DNNs) using VGG-16 and AlexNet reported an accuracy of 92%. More recent architectures, such as the GoogLeNet combined with AlexNet, improved performance significantly, reaching 97.84% accuracy. The proposed model demonstrates superior or highly competitive performance in terms of accuracy. It achieves the highest accuracy (98.10%), precision (83.65%), F1-score (90.35%), and specificity (98.57%) among all compared methods. The usefulness of integrating detection and classification for DS analysis was confirmed by the suggested YOLOv8 ensemble framework, which consistently exceeded earlier deep learning and traditional benchmarks, achieving the greatest accuracy of 98.10%. However, a limitation is that NT was approximated via bounding box height rather than anatomical boundary segmentation, which may not perfectly align with anatomical boundaries. Future work can address this limitation by implementing true segmentation-based refinement.

Table 5. Evaluation of the proposed approach against current approaches

Method	Accuracy (%)	Precision (%)	F1-score (%)	Specificity (%)	Recall (%)
DNN (VGG-16 and AlexNet) [33]	92.00	–	–	86.00	100.00
Chan-Vese based [49]	90.00	77.00	82.00	91.00	87.00
Hierarchical structural model [27]	94.00	84.00	89.00	94.00	96.00
GoogLeNet + AlexNet [37]	97.84	96.04	97.80	96.04	99.64
Proposed (YOLOv8 + ensemble framework)	98.10	83.65	90.35	98.57	97.64

In medical imaging, the lack of vast and varied datasets continues to be a major challenge, frequently restricting the generalization potential of deep learning models. To address this implemented a transfer learning approach that allowed knowledge transfer from networks that had already been trained. Despite the small quantity of the sample, the proposed method detected DS with a remarkable degree of accuracy.

The proposed framework yields clinically interpretable results with accurate localization of the NTs and visualization of the Grad-CAM—showing that the model is focused on clinically relevant anatomical features. NT is a known first trimester biomarker for prenatal screening of chromosomal abnormalities, especially DS. Other fetal abnormalities, including congenital cardiac defects, are also associated with increased NT thickness indicating the clinical relevance of the accurate localization of NT for early risk stratification and prompt referral for further diagnostic assessment. Automated NT analysis will be more reliable because there is less variation in one clinician's measurements across time and among different clinicians, and more reproducible (consistent) clinical assessments. The proposed deep learning framework is also time efficient, easy to implement and can be seamlessly integrated into the first trimester ultrasound workflow as a decision support tool. The framework can be embedded in clinical systems of hospital ultrasound to automatically locate the NT region and to calculate the DS risk in real-time during normal screening procedures. The generated Grad-CAM visualizations can also help clinicians interpret the model as they can see what parts of the image are important to the model's prediction and improve its transparency. The framework facilitates early risk stratification and NT region localization and ensures expert clinical supervision, helping clinicians enhance diagnostic accuracy and efficiency and ultimately leading to timely interventions. The proposed framework is meant to work in tandem with, and not in place of, clinical expert judgment and is meant for ease of use in the pragmatic implementation of routine prenatal screening.

Despite its high performance in the localization of NT and classification of DS, the robustness of the proposed YOLOv8 + Ensemble under different ultrasound acquisition conditions (noise, position, and ultrasound device) was not investigated in the present study. Thus, the framework proposed herein needs to be further studied for its generalizability in a variety of clinical environments. Comprehensive robustness evaluation of these multi-center datasets collected with different imaging conditions will be the subject of future research.

5. CONCLUSION

This study proposed a deep learning architecture for improving the prenatal screening of DS. It employed YOLOv8 to accurately locate NT areas on sonographic images. To enhance the diagnostic accuracy, the three models ResNet50, DenseNet201, and EfficientNet-B4 are combined in an ensembled model to classify fetuses as healthy or DS. The results presented excellent specificity, sensitivity, and accuracy. The advantages of automatic detection coupled with ensemble classification were validated by the performance of the proposed system that significantly outperformed the existing benchmarks over the previous deep learning systems and traditional image processing approaches. Future research will focus on verifying the proposed methodology on larger multi-center datasets acquired under diverse ultrasound conditions, including variations in image quality, fetal position, and ultrasound devices, to further improve its robustness and clinical applicability.

FUNDING INFORMATION

Authors state no funding involved.

AUTHOR CONTRIBUTIONS STATEMEN

This journal uses the Contributor Roles Taxonomy (CRediT) to recognize individual author contributions, reduce authorship disputes, and facilitate collaboration.

Name of Author	C	M	So	Va	Fo	I	R	D	O	E	Vi	Su	P	Fu
Sandip Rajendra Aher	✓	✓	✓	✓	✓	✓		✓	✓	✓	✓			
Balasaheb Shrirangrao Agarkar	✓	✓				✓		✓	✓	✓	✓	✓		
Sachin Vasant Chaudhari	✓	✓				✓			✓	✓	✓			

C : **C**onceptualization
M : **M**ethodology
So : **So**ftware
Va : **Va**lidation
Fo : **Fo**rmal Analysis
I : **I**nvestigation
R : **R**esources
D : **D**ata Curation
O : Writing - **O**riginal Draft
E : Writing - Review & **E**diting
Vi : **Vi**sualization
Su : **Su**pervision
P : **P**roject Administration
Fu : **Fu**nding Acquisition

CONFLICT OF INTEREST STATEMENT

Authors state no conflict of interest.

DATA AVAILABILITY

The supporting data of this study are openly available in Mendeley Data at http://doi.org/10.17632/n2rbrb9t4f.1, reference number [47].

REFERENCES

[1] S. E. Antonarakis *et al*., "Down syndrome," *Nature Reviews Disease Primers*, vol. 6, no. 1, Feb. 2020, doi: 10.1038/s41572-019-0143-7.

[2] S. L. Sherman, E. G. Allen, L. H. Bean, and S. B. Freeman, "Epidemiology of down syndrome," *Mental Retardation and Developmental Disabilities Research Reviews*, vol. 13, no. 3, pp. 221–227, Jan. 2007, doi: 10.1002/mrdd.20157.

[3] Y.-B. Lee, M.-J. Kim, and M.-H. Kim, "Robust border enhancement and detection for measurement of fetal nuchal translucency in ultrasound images," *Medical & Biological Engineering & Computing*, vol. 45, no. 11, pp. 1143–1152, Nov. 2007, doi: 10.1007/s11517-007-0225-7.

[4] N. J. Wald, L. George, D. Smith, J. W. Densem, and K. Pettersonm, "Serum screening for down's syndrome between 8 and 14 weeks of pregnancy," *BJOG: An International Journal of Obstetrics & Gynaecology*, vol. 103, no. 5, pp. 407–412, May 1996, doi: 10.1111/j.1471-0528.1996.tb09765.x.

[5] M. C. Thomas, S. P. Arjunan, and R. Viswanathan, "Nuchal translucency thickness measurement in fetal ultrasound images to analyze down syndrome," *IETE Journal of Research*, vol. 69, no. 8, pp. 4989–4999, Sep. 2023, doi: 10.1080/03772063.2021.1972847.

[6] C. Suwanrath, N. Pruksanusak, O. K.-Anantakul, T. Suntharasaj, T. Hanprasertpong, and S. Pranpanus, "Reliability of fetal nasal bone length measurement at 11–14 weeks of gestation," *BMC Pregnancy and Childbirth*, vol. 13, no. 1, Dec. 2013, doi: 10.1186/1471-2393-13-7.

[7] J. Moratalla, K. Pintoffl, R. Minekawa, R. Lachmann, D. Wright, and K. H. Nicolaides, "Semi-automated system for measurement of nuchal translucency thickness," *Ultrasound in Obstetrics & Gynecology*, vol. 36, no. 4, pp. 412–416, Oct. 2010, doi: 10.1002/uog.7737.

[8] S. Nie, J. Yu, P. Chen, Y. Wang, and J. Q. Zhang, "Automatic detection of standard sagittal plane in the first trimester of pregnancy using 3-D ultrasound data," *Ultrasound in Medicine & Biology*, vol. 43, no. 1, pp. 286–300, Jan. 2017, doi: 10.1016/j.ultrasmedbio.2016.08.034.

[9] H. Y. Cho *et al*., "Comparison of nuchal translucency measurements obtained using volume NT TM and two- and three-dimensional ultrasound," *Ultrasound in Obstetrics & Gynecology*, vol. 39, no. 2, pp. 175–180, Feb. 2012, doi: 10.1002/uog.8996.

[10] M. A. Müller, E. Pajkrt, O. P. Bleker, G. J. Bonsel, and C. M. Bilardo, "Disappearance of enlarged nuchal translucency before 14 weeks' gestation: relationship with chromosomal abnormalities and pregnancy outcome," *Ultrasound in Obstetrics & Gynecology*, vol. 24, no. 2, pp. 169–174, Aug. 2004, doi: 10.1002/uog.1103.

[11] F. Orlandi *et al*., "Measurement of nasal bone length at 11–14 weeks of pregnancy and its potential role in down syndrome risk assessment," *Ultrasound in Obstetrics & Gynecology*, vol. 22, no. 1, pp. 36–39, Jul. 2003, doi: 10.1002/uog.167.

[12] B. B. Bet, M. A. Lugthart, I. H. Linskens, M. C. van Maarle, E. van Leeuwen, and E. Pajkrt, "Adverse pregnancy outcome in fetuses with early increased nuchal translucency: prospective cohort study," *Ultrasound in Obstetrics & Gynecology*, vol. 64, no. 2, pp. 164–172, Aug. 2024, doi: 10.1002/uog.27623.

[13] K. H. Nicolaides, G. Azar, D. Byrne, C. Mansur, and K. Marks, "Fetal nuchal translucency: ultrasound screening for chromosomal defects in first trimester of pregnancy," *British Medical Journal*, vol. 304, no. 6831, pp. 867–869, Apr. 1992, doi: 10.1136/bmj.304.6831.867.

[14] M. Westin, S. Saltvedt, G. Bergman, H. Almström, C. Grunewald, and L. Valentin, "Is measurement of nuchal translucency thickness a useful screening tool for heart defects? A study of 16 383 fetuses," *Ultrasound in Obstetrics & Gynecology*, vol. 27, no. 6, pp. 632–639, Jun. 2006, doi: 10.1002/uog.2792.

[15] K. O. Kagan, K. Avgidou, F. S. Molina, K. Gajewska, and K. H. Nicolaides, "Relation between increased fetal nuchal translucency thickness and chromosomal defects," *Obstetrics & Gynecology*, vol. 107, no. 1, pp. 6–10, Jan. 2006, doi: 10.1097/01.AOG.0000191301.63871.c6.

[16] F. Bernardino, R. Cardoso, N. Montenegro, J. Bernardes, and J. M. de Sa, "Semiautomated ultrasonographic measurement of fetal nuchal translucency using a computer software tool," *Ultrasound in Medicine & Biology*, vol. 24, no. 1, pp. 51–54, Jan. 1998, doi: 10.1016/S0301-5629(97)00235-4.

[17] S. Aher, B. Agarkar, and S. Chaudhari, "A comprehensive survey on nuchal translucency segmentation and thickness estimation," in *2024 International Conference on Inventive Computation Technologies (ICICT)*, Apr. 2024, pp. 327–334. doi: 10.1109/ICICT60155.2024.10544844.

[18] G. Sciortino, D. Tegolo, and C. Valenti, "Automatic detection and measurement of nuchal translucency," *Computers in Biology and Medicine*, vol. 82, pp. 12–20, Mar. 2017, doi: 10.1016/j.compbiomed.2017.01.008.

[19] R. Varghese and S. M., "YOLOv8: a novel object detection algorithm with enhanced performance and robustness," in *2024 International Conference on Advances in Data Engineering and Intelligent Computing Systems (ADICS)*, Apr. 2024, pp. 1–6, doi: 10.1109/ADICS58448.2024.10533619.

[20] Iqra and K. J. Giri, "SO-YOLOv8: a novel deep learning-based approach for small object detection with YOLO beyond COCO," *Expert Systems with Applications*, vol. 280, Jun. 2025, doi: 10.1016/j.eswa.2025.127447.

[21] J. Wan, B. Li, K. Wang, X. Teng, T. Wang, and B. Mao, "An improved ResNet50 for environment image classification," *Procedia Computer Science*, vol. 242, pp. 1000–1007, 2024, doi: 10.1016/j.procs.2024.08.246.

[22] R. A. Charisma and F. D. Adhinata, "Transfer learning with DenseNet201 architecture model for potato leaf disease classification," in *2023 International Conference on Computer Science, Information Technology and Engineering (ICCoSITE)*, Feb. 2023, pp. 738–743, doi: 10.1109/ICCoSITE57641.2023.10127772.
[23] S. Srinivasan and K. Rajakumar, "Hyperspectral image classification using efficientnet-B4 with search and rescue operation algorithm," *International Journal of Information Technology*, vol. 15, no. 3, pp. 1473–1479, Mar. 2023, doi: 10.1007/s41870-023-01197-8.
[24] E. Catanzariti, G. Fusco, F. Isgrò, S. Masecchia, R. Prevete, and M. Santoro, "A semi-automated method for the measurement of the fetal nuchal translucency in ultrasound images," in *Image Analysis and Processing – ICIAP 2009*, Berlin, Heidelberg: Springer, 2009, pp. 613–622, doi: 10.1007/978-3-642-04146-4_66.
[25] S. Nirmala and V. Palanisamy, "Measurement of nuchal translucency thickness in first trimester ultrasound fetal images for detection of chromosomal abnormalities," in *2009 International Conference on Control, Automation, Communication and Energy Conservation*, 2009, pp. 1–5.
[26] Y.-H. Deng, Y.-Y. Wang, and P. Chen, "Estimating fetal nuchal translucency parameters from its ultrasound image," in *2008 2nd International Conference on Bioinformatics and Biomedical Engineering*, May 2008, pp. 2643–2646, doi: 10.1109/ICBBE.2008.994.
[27] Y. Deng, Y. Wang, and P. Chen, "Automated detection of fetal nuchal translucency based on hierarchical structural model," in *2010 IEEE 23rd International Symposium on Computer-Based Medical Systems (CBMS)*, Oct. 2010, pp. 78–84, doi: 10.1109/CBMS.2010.6042618.
[28] Y. Deng, Y. Wang, P. Chen, and J. Yu, "A hierarchical model for automatic nuchal translucency detection from ultrasound images," *Computers in Biology and Medicine*, vol. 42, no. 6, pp. 706–713, Jun. 2012, doi: 10.1016/j.compbiomed.2012.04.002.
[29] E. Supriyanto, L. K. Wee, and T. Y. Min, "Ultrasonic marker pattern recognition and measurement using artificial neural network," in *Proceedings of the 9th WSEAS international conference on Signal processing*, 2010, pp. 35–40.
[30] J. Park, M. Sofka, S. Lee, D. Kim, and S. K. Zhou, "Automatic nuchal translucency measurement from ultrasonography," in *Medical Image Computing and Computer-Assisted Intervention – MICCAI 2013*, Berlin, Heidelberg: Springer, 2013, pp. 243–250, doi: 10.1007/978-3-642-40760-4_31.
[31] R. Sonia and V. Shanthi, "Image classification for ultrasound fetal images with increased nuchal translucency during first trimester using SVM classifier," *Research Journal of Applied Sciences, Engineering and Technology*, vol. 9, no. 2, pp. 113–121, Jan. 2015, doi: 10.19026/rjaset.9.1385.
[32] A. Anzalone *et al.*, "A system for the automatic measurement of the nuchal translucency thickness from ultrasound video stream of the foetus," in *Proceedings of the 26th IEEE International Symposium on Computer-Based Medical Systems*, Jun. 2013, pp. 239–244, doi: 10.1109/CBMS.2013.6627795.
[33] M. C. Thomas and S. P. Arjunan, "Deep learning measurement model to segment the nuchal translucency region for the early identification of down syndrome," *Measurement Science Review*, vol. 22, no. 4, pp. 187–192, Aug. 2022, doi: 10.2478/msr-2022-0023.
[34] K. Chaudhari and S. Oza, "Ultrasound image based fully-automated nuchal translucency segmentation and thickness measurement," *International Journal of Nonlinear Analysis and Applications*, vol. 12, Special Issue, pp. 1573–1583, 2021, doi: 10.22075/ijnaa.2021.5830.
[35] V. Devi and R. Ramachandran, "Down syndrome detection using modified AdaBoost algorithm," *International Journal of Electrical and Computer Engineering*, vol. 11, no. 5, pp. 4281–4288, Oct. 2021, doi: 10.11591/ijece.v11i5.pp4281-4288.
[36] T. Liu *et al.*, "Direct detection and measurement of nuchal translucency with neural networks from ultrasound images," in *Smart Ultrasound Imaging and Perinatal, Preterm and Paediatric Image Analysis*, Cham: Springer, 2019, pp. 20–28, doi: 10.1007/978-3-030-32875-7_3.
[37] S. R. Aher, B. S. Agarkar, and S. V. Chaudhari, "Deep learning approach for segmenting nuchal translucency region in fetal ultrasound images for detecting down syndrome using GoogLeNet and AlexNet," *Journal of Electronics, Electromedical Engineering, and Medical Informatics*, vol. 7, no. 2, pp. 450–459, Apr. 2025, doi: 10.35882/jeeemi.v7i2.729.
[38] L. Zhang *et al.*, "Development and validation of a deep learning model to screen for trisomy 21 during the first trimester from nuchal ultrasonographic images," *JAMA Network Open*, vol. 5, no. 6, Jun. 2022, doi: 10.1001/jamanetworkopen.2022.17854.
[39] B. Kasera *et al.*, "Deep-learning computer vision can identify increased nuchal translucency in the first trimester of pregnancy," *Prenatal Diagnosis*, vol. 44, no. 5, pp. 535–543, May 2024, doi: 10.1002/pd.6559.
[40] L. Liu *et al.*, "Intelligent quality assessment of ultrasound images for fetal nuchal translucency measurement during the first trimester of pregnancy based on deep learning models," *BMC Pregnancy and Childbirth*, vol. 25, no. 1, Jul. 2025, doi: 10.1186/s12884-025-07863-y.
[41] L. Zhao *et al.*, "Deep content and contrastive perception learning for automatic fetal nuchal translucency image quality assessment," *Engineering Applications of Artificial Intelligence*, vol. 152, Jul. 2025, doi: 10.1016/j.engappai.2025.110687.
[42] C.-Y. Chen *et al.*, "Developing a transfer learning model for the prediction of down syndrome from first-trimester ultrasound images," *Taiwanese Journal of Obstetrics and Gynecology*, vol. 64, no. 6, pp. 1017–1023, Nov. 2025, doi: 10.1016/j.tjog.2025.08.001.
[43] H. D. Do *et al.*, "Applying machine learning in screening for down syndrome in both trimesters for diverse healthcare scenarios," *Heliyon*, vol. 10, no. 15, Aug. 2024, doi: 10.1016/j.heliyon.2024.e34476.
[44] Y. Zhang *et al.*, "Deep learning model for real-time nuchal translucency assessment at Prenatal US," *Radiology: Artificial Intelligence*, vol. 7, no. 4, Jul. 2025, doi: 10.1148/ryai.240498.
[45] H. Kwon, H. Hur, H. C. Cho, Y. ji Jung, S. Kim, and J. Kwon, "Feasibility and reproducibility of a structure-guided deep learning model for automatic detection of the standard sagittal plane in first-trimester nuchal translucency assessment using 3D ultrasound," *Journal of Ultrasound in Medicine*, vol. 45, no. 10, pp. 2165–2173, Oct. 2026, doi: 10.1002/jum.70281.
[46] R. O. Baddad, A. Y. Owda, and M. Owda, "A deep learning framework for ultrasound image quality assessment and automated nuchal translucency measurement to improve first-trimester chromosomal abnormality screening," *AI*, vol. 7, no. 2, Feb. 2026, doi: 10.3390/ai7020045.
[47] C. Cui and F. Dong, "Dataset for fetus framework," *Mendeley Data*, vol. 1, 2022, doi: 10.17632/n2rbrb9t4f.1.

[48] P. Zhou, X. Xie, Z. Lin, and S. Yan, "Towards understanding convergence and generalization of AdamW," *IEEE Transactions on Pattern Analysis and Machine Intelligence*, vol. 46, no. 9, pp. 6486–6493, Sep. 2024, doi: 10.1109/TPAMI.2024.3382294.
[49] M. C. Thomas and S. P. Arjunan, "Identification and segmentation of nuchal translucency region during the early stages of gestation using chan-vese segmentation," in *2021 International Conference on Computer Communication and Informatics (ICCCI)*, Jan. 2021, pp. 1–5, doi: 10.1109/ICCCI50826.2021.9402299.

BIOGRAPHIES OF AUTHORS



Sandip Rajendra Aher received the bachelor's degree in Electronics Engineering from Savitribai Phule Pune University in the year 2011. He earned his master's degree in VLSI and Embedded Systems from Savitribai Phule Pune University in the year 2014. He has 14 years of teaching experience as assistant professor at Pravara Rural Engineering College, Loni. Currently he is a research scholar in the Department of Electronics and Telecommunication at Sanjivani College of Engineering, which is affiliated with Savitribai Phule Pune University. His research interests include machine learning, deep learning, computer vision and biomedical electronics. He is also working on deep learning based biomedical projects on image processing. He can be contacted at email: sandip.aher1719@gmail.com.



Dr. Balasaheb Shrirangrao Agarkar holds a Ph.D. in Electronics Engineering from Swami Ramanand Teerth Marathwada University, Nanded (India), received in 2016. He received a bachelor's degree (B.E.) in Electronics Engineering and a master's (M. Tech.) in Electronics Design Technology from Dr. Babasaheb Ambedkar Matathwada University, Chh. Sambhajinagar (India) in 1990 and 1998 respectively. Currently, he is working as a professor in the Department of Electronics and Computer Engineering, Sanjivani College of Engineering, Kopargaon, India. He is a member of the board of studies (BoS) and a research guide in Electronics and Telecommunication Engineering at Savitribai Phule Pune University, Pune, India. His area of research interests are computer networks, packet classification algorithms, artificial neural networks, neuro-fuzzy systems, image processing. He has published 12 research papers in international journals. He can be contacted at email: bsagarkar977@gmail.com.



Dr. Sachin Vasant Chaudhari is a Ph.D. holder in Electronics Engineering. He is an associate professor in the Electronics and Telecommunication Engineering Department at Sanjivani College of Engineering, Kopargaon, which is affiliated with Savitribai Phule Pune University, Pune, India. He has worked on a broad range of topics including automated deep learning, UAV route planning, hybrid energy systems, and medical applications. His innovative research also addresses dynamic routing algorithms, channel estimation in OFDM, and advanced materials for medical implants. He has published over 35 papers in reputed international journals. He is having professional membership of the Institution of Engineers (IEI) and International Association of Engineers (IANG). He can be contacted at email: chaudharisachinetc@sanjivani.org.in.